Materials Research Express

Lifetime, quasi-Fermi level splitting and doping concentration of Cu-rich $CuInS_2$ absorbers

To cite this article: Damilola Adeleye *et al* 2021 *Mater. Res. Express* **8** 025905

IOP Publishing *Mater. Res. Express* **8** (2021) 025905 https://doi.org/10.1088/2053-1591/abe3c1

Materials Research Express

CrossMark

OPEN ACCESS

RECEIVED
17 December 2020

REVISED
14 January 2021

ACCEPTED FOR PUBLICATION
5 February 2021

PUBLISHED
17 February 2021

PAPER

Lifetime, quasi-Fermi level splitting and doping concentration of Cu-rich $CuInS_2$ absorbers

Damilola Adeleye , Alberto Lomuscio , Mohit Sood and Susanne Siebentritt

Laboratory for Photovoltaics, Department of Physics and Materials Science, University of Luxembourg, L-4422 Belvaux, Luxembourg

E-mail: damilola.adeleye@uni.lu

Keywords: $Cu(In,Ga)S_2$, quasi-Fermi level splitting, lifetime, doping concentration, photoluminescence, optoelectronics, carrier generation and recombination

Abstract

Cu(In,Ga)S2–based solar cells have been shown by Hiroi *et al* (Hiroi *et al* 2015 *IEEE Journal of Photovoltaics* **6** 309–312) to achieve higher efficiencies with absorbers processed at high deposition temperatures. Additionally, it is known for $CuInS_2$ cells that the main improvement from higher deposition temperatures is the reduction in the density of deep defects and increased quasi-Fermi level splitting. The increased quasi-Fermi level splitting could result from a reduction in the rate of recombination or from an increase in doping concentration. To investigate which effect is the dominant one, we perform time-resolved photoluminescence measurements and estimate the doping concentration from carrier lifetime and quasi-Fermi level splitting. We find no changes in the effective lifetime, which is in the range of 200 ps. The doping concentration increases from 10^{16} cm^{-3} to 10^{17} cm^{-3}. Our study shows that the increase in quasi-Fermi level splitting with higher deposition temperatures is not due to reduction in non-radiative recombination but due to increased doping concentration.

1. Introduction

Copper indium gallium disulfide, $Cu(In,Ga)S_2$, is among the chalcopyrite materials which promise stable high-efficiency photovoltaic applications. Its bandgap tunability from ~1.55 eV [1] (in pure $CuInS_2$) to ~2.45 eV [1] (in pure $CuGaS_2$) provides suitable values for use as a single-junction solar cell or in tandem with other absorbers for a multijunction solar cell [2, 3]. In comparison to its selenide counterpart, $Cu(In,Ga)S_2$ still suffers from a high open circuit voltage deficit, that is, voltage loss relative to bandgap, ~600 mV compared to ~360 mV in $Cu(In,Ga)Se_2$ [4, 5]. However, Hiroi *et al* have achieved a high efficiency $Cu(In,Ga)S_2$ solar cell with absorbers processed at high temperature deposition [4, 6]. To understand the influence of the deposition temperature, previously, we have shown, for $CuInS_2$ (without Ga), that the main enhancement from a higher deposition temperature stems from reduced non-radiative recombination in the absorber, because we observed an increased quasi-Fermi level splitting with higher deposition temperature (QFLS) [7, 8]. Additionally, we have shown that for a set deposition temperature, there is an increase in QFLS with higher Cu-excess, i.e., integral composition of $[Cu]/[In] > 1$ [7, 8]. We could show that the higher QFLS goes along with the reduction of a deep defect [7]. Therefore, it was assumed that the QLFS improvement is due to the reduced density of recombination centres, which would increase the minority carrier lifetime. QFLS gives insight into the quality of the absorber without and before the intricacies of completing the device. As such, it serves as an upper limit for the open circuit voltage in solar cell devices [9, 10].

The minority carrier lifetime is one of the essential parameters used for characterizing doped semiconductor materials for solar cell [11]. It is a measure of device quality by quantifying the rate of recombination and it is directly related to device efficiency [12–14]. $Cu(In,Ga)S_2$ features very short lifetimes of hundred picoseconds [15] when compared to $Cu(In,Ga)Se_2$ where lifetime can range from tens to hundreds of nanoseconds [13, 14, 16]. Longer minority carrier lifetimes indicate a higher concentration of minority carriers and thus a higher electron Fermi level $E_{F,C}$, which in turn increases the QFLS.

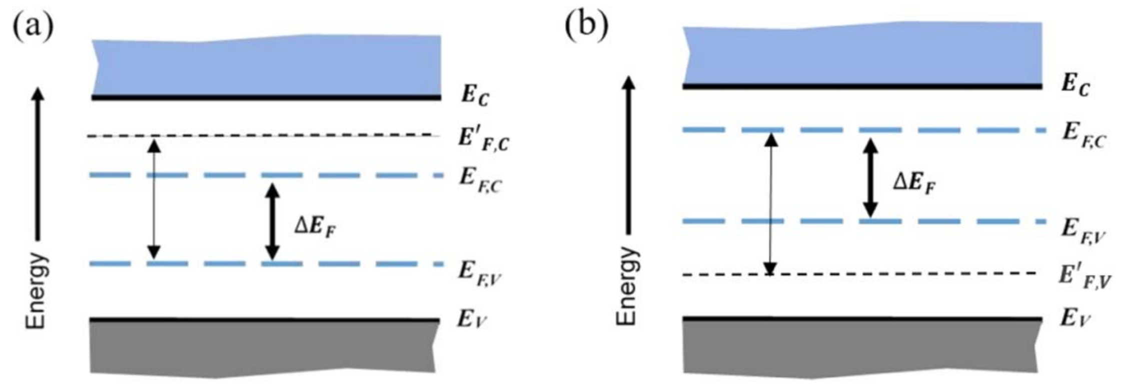

Figure 1. Illustration of the positions of the Fermi energy levels with respect to: (a) a reduction of recombination centres (higher electron quasi Fermi level) (b) higher doping concentration (lower hole Fermi level).

The dependence of many device properties and performance on doping concentration makes it an important material property. Established techniques of obtaining the dopant concentration in thin-film solar cells include capacitance−voltage (CV) measurements or Hall measurements [17–19]. Doping concentration has a strong influence on the QFLS of an absorber. In a p-type $CuInS_2$ absorber, with a higher number of acceptors than donors, any changes in doping concentration would change the position of the hole Fermi level ($E_{F,V}$), thereby changing the QFLS. The effect of changes in Fermi levels with changes in the density if recombination centres or doping level, which in turn results in changes in QFLS, are illustrated in figure 1. In figure 1(a) shows the case of a reduced density of recombination centres: with the Fermi levels split, the position of the electron Fermi level $E_{F,C}$ would shift higher to $E'_{F,C}$ as shown here—and it is assumed that everything else remain unchanged. This would in turn increase the QFLS. Rather, as shown in figure 1(b), as the doping concentration increases and no change in the density of recombination centres, the hole Fermi level ($E_{F,V}$) moves closer to the valence band, thereby increasing the QFLS.

In this paper, the cause of the improvement in QFLS with growth temperature and Cu content for Cu-rich $CuInS_2$ absorbers by means of photoluminescence measurements is probed [9, 20]. By using information derived from time-resolved and calibrated photoluminescence (PL) measurements, which yield the effective minority carrier lifetime and QFLS respectively, we investigate if the improved QFLS is due to less recombination or higher doping concentration. All PL measurements are excited by a laser that is absorbed within the first nm of the μm thick films, thus an influence of differences in the absorptivity can be excluded.

2. Preparation of samples and details of experimental produres

The absorber layers studied were deposited by co-evaporation under Cu excess condition i.e., integral composition of $[Cu]/[In] > 1$, denoted as Cu-rich. The absorbers form stoichiometric $CuInS_2$ with Cu/In ratio ≈ 1, and copper sulfide (Cu_xS) secondary phases [21]. The Cu_xS phase was removed by potassium cyanide (KCN) etching leaving an almost stoichiometric absorber [21]. Details of the deposition process can be found in reports by Lomuscio *et al* [7, 8]. Unlike the selenides, e.g. $CuInSe_2$, the absorbers do not degrade in air and did not require cadmium sulfide (CdS) coating to prevent degradation [7, 22]. In time-resolved photoluminescence (TRPL) measurement, a laser pulse excites electron-hole pairs in the absorber and the photoluminescence is recorded in time. The TRPL measurements were performed by time-correlated single photon counting (TCSPC) [23]. Excitation was supplied by an 85 ps pulsed laser of 638 nm wavelength at a repetition rate (f_{rep}) of 20 MHz. The diameter of the focused beam was ~45 μm. The PL emission was detected with a high-speed photomultiplier with an integrated amplifier. As illustrated in figure 2(a), all measurements were at the PL emission peak ~820 nm, with the integrated monochromator bandwidth of 45 nm to accumulate an adequate number of photons for all the samples at the same measurement condition. The number of excess minority carriers was approximately 7.6×10^{16} cm^{-3}. This is determined by calculating the number of photons per pulse, assuming that all the photons are absorbed and generate excess carrier pairs, which are then evenly distributed over the absorption length. That is, $\Delta n = \alpha \cdot P_0/(f_{rep} * A_{beam} * E_{photon})$, where Δn, α, P_0, f_{rep}, A_{beam} and E_{photon} is the excess minority carriers, absorption coefficient, average laser power, repetition rate, beam area and photon energy respectively. The absorption coefficient of $CuInS_2$ at the wavelength of the pulsed laser, was estimated as 6.5×10^4 cm^{-1} [24]. We aim at low injection conditions, where the excess carrier concentration (Δn) is less than the equilibrium hole density (p_0), i.e. $\Delta n \ll p_0$, because in this case the PL decay time is solely determined by the minority carrier lifetime [25]. On the other hand, in a high injection condition

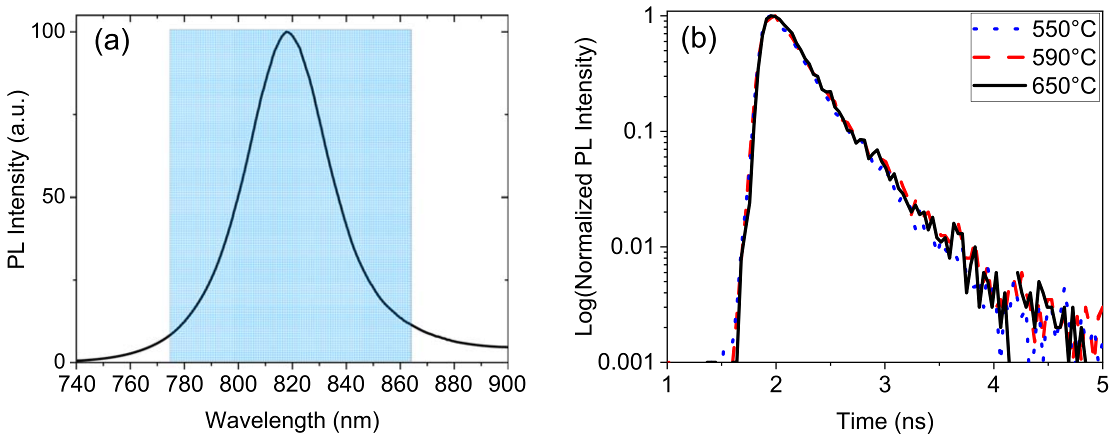

Figure 2. Exemplary photoluminescence curves. (a) Spectrum of a Cu-rich CIS showing the range accounted for by the monochromator bandwidth. (b) Normalized measured time-resolved decays on absorbers with growth temperature of 550 °C (dotted line), 590 °C (dashed line) and 650 °C (solid line).

$\Delta n \gg p_0$ and the PL decay time is determined by both, minority and majority carrier lifetimes [11, 25]. In this work, the excess carrier density is close to the low-injection condition, lower than the typical doping concentration of $\sim 10^{17}$ cm^{-3} for Cu-rich CuInS$_2$ [26, 27]. Excitations at lower injection levels were not possible due to the weak luminescence of the absorbers, which led to a low signal to noise ratio. To account for uncertainty in TCSPC, we also measure the instrument response function (IRF) of the set-up. The measured decay curve, $M(t)$ is a convolution in time t of the luminescence decay $D(t)$ and the $IRF(t)$, i.e., $M(t) = \int_0^t IRF(t')D(t - t')\mathrm{d}t'$ [26]. The luminescence decay $D(t)$ is recovered and fitted using a commercial software from Edinburgh Instruments.

The luminescence decay for an ideal semiconductor is characterized by a single exponential decay [11]. However, CIGS absorbers often feature a multi-exponential decay which can be described as an overlay of several decay times [14]. In this work, background signal from the dark counts are subtracted, after which the effective lifetime is extracted from the luminescence decay curve by a triple-exponential fit

$$I_{PL}(t) = \sum_i A_i \exp\left(-\frac{t}{\tau_i}\right) \tag{1}$$

where $I_{PL}(t)$ is the intensity at a time t after the laser pulse, A_i decay amplitude and τ_i the decay times for each $i = 1, 2, 3$. The effective lifetime is then a weighted-average τ_{amp} defined as, $\tau_{amp} = \sum_i A_i\tau_i / \sum_i A_i$ [28]. The weighted-average method takes does not give information of the different decay channels, but it allows for a comparison of samples.

For a calibrated measurement to determine the QFLS, the PL experiment is performed using a 660 nm continuous-wave (CW) laser for optical excitation. Two corrections, namely spectral and intensity, are applied to the raw PL data measured by a steady state excitation. The spectral correction is applied with a commercial calibrated halogen lamp. The intensity correction entails the measurement of the laser beam diameter with a charged-couple device (CCD) camera and the laser power by a photodiode power meter. The incident photon flux is then calculated, and adapted to twice the AM 1.5 solar spectrum photon flux above the bandgap. The room-temperature bandgap for the samples was ~1.51 eV. An illumination of '1 suns' is used on the samples. The corrected (and now calibrated) spectra are transformed to the energy domain and evaluated using Planck's generalized law [29], which describes the energy dependence of the PL yield as a function of absorptivity, temperature, and QFLS. The QFLS is extracted from a fit of the sufficiently high-energy wing of the PL spectra where absorptivity is assumed to be unity [9]. More details on QFLS evaluation can be found in the supplemental detail reported by Babbe *et al* [30].

3. Results and discussion

3.1. Effect of changes in growth temperature on the QFLS and effective lifetime

The influence of the integral composition and growth temperature on quasi-Fermi level splitting of Cu-rich CIS absorbers have been reported by Lomuscio *et al* [8]. The results of the different growth parameters and composition on lifetime are presented and discussed here.

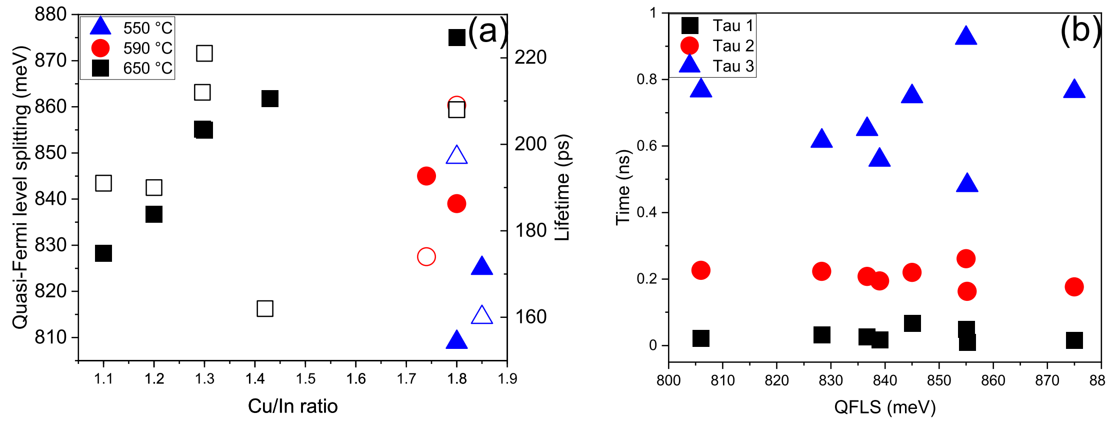

Figure 3. (a) QFLS (filled) and lifetime (open) plotted against Cu/In ratio for absorbers with different growth temperatures of 550 °C (blue), 590 °C (red) and 650 °C (black). The quasi-Fermi level splitting data of growth temperature 650 °C has been shown previously by Lomuscio *et al* [8]. (b) The distribution of the different decay times τ_1, τ_2 and τ_3 are plotted against QFLS.

Table 1. Summary of the QFLS and lifetime on absorbers with [Cu]/[In] = 1.8.

Sample	Growth temperature	QFLS	Lifetime
A	550 °C	806 meV	197 ± 35 ps
B	590 °C	839 meV	209 ± 32 ps
C	650 °C	875 meV	208 ± 33 ps

To investigate the impact of growth temperature on the rate of recombination, lifetime measurement were carried out on three absorbers with similar Cu/In ratio of 1.8, but different growth temperatures of 550 °C, 590 °C and 650 °C. The decay curves are shown in figure 2(b). It can be seen that, there is no change in the decay curves for the three absorbers. Upon evaluation, the extracted lifetime is about 200 ps. This is an indication of a faster rate of recombination in the CIS absorbers compared to the selenides. Nonetheless, the similarity in the effective lifetime shows that the difference in growth temperature has no significant influence on the rate of recombination of minority carriers in the different absorbers. Details of the QFLS and lifetime of the absorbers are presented in table 1.

From table 1, it is seen that there is a clear increase in QFLS with increasing growth temperature, but the lifetime does not change.

3.2. Quasi-Fermi level splitting and effective lifetime on absorbers with different composition

The dependence of QFLS on Cu/In has also been reported by Lomuscio *et al* [8]. It was shown that there is an increase in QFLS with higher Cu-excess. Here, the Cu-rich absorbers with a Cu/In ratio from about 1.1 to 1.8 are investigated. In figure 3(a), the QFLS and the effective lifetimes are plotted against the corresponding Cu/In ratio. For absorbers processed at 650 °C (black dots), there is a clear increase of more than 40 meV in QFLS with increasing Cu/In ratio, but the lifetime does not show a corresponding increase. In fact, the lifetime scatters around 200 ps. For the high Cu/In ratios different growth temperatures are shown. Again, the QFLS increases with growth temperature, whereas the lifetimes scatter around 190 ps.

The origin of this indiscriminate distribution becomes obvious in figure 3(b) where the decay times τ_1, τ_2 and τ_3 are plotted with respect to the QFLS measured on the same sample. The times τ_1 and τ_2 are ~30 ps and ~200 ps respectively and not correlated with QFLS. τ_1 and τ_2 are responsible for the main part of the observed decays. τ_3 arises from the decay tail where the influence of noise becomes much more important and thus τ_3 even more randomly distributed between 400 ps and 800 ps. Regardless of the growth temperature or Cu/In of the absorbers studied, the lifetime is always the same. This indicates that, the improved QFLS is not due to reduction in the rate of recombination. Thus, an increase in doping with higher Cu/In ratios or higher growth temperatures must be the reason for the increase in QFLS.

3.3. Effect of doping level on the quasi-Fermi level splitting

Here, the effect of doping concentration on QFLS is studied. The estimation of doping concentration from the measurement of the QFLS and the lifetime is described. In a p-type absorber where the majority carrier are holes, the minority carrier can be generated by an external source, and it is possible to estimate the electron

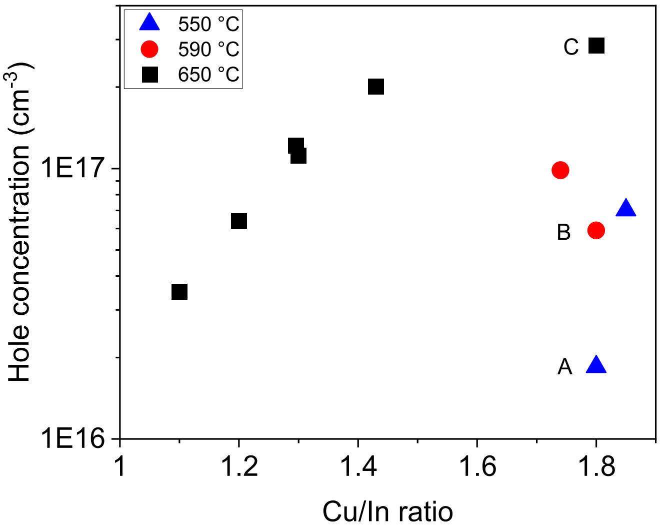

Figure 4. Estimated doping concentration on the different absorbers plotted against the Cu/In ratio. The absorbers labelled A, B and C with Cu/In ratio of 1.8 were processed at temperatures of 550 °C, 590 °C and 650 °C respectively.

concentration from the photon flux (ϕ) on the absorber. Since the QFLS is measured under steady state excitation, the generation rate is considered for a steady state light source. For the excitation source, it is assumed that every photon is absorbed and generates an electron-hole pair. Then the excess carrier concentration can be determined from the lifetime. Assuming that the diffusion length of the charge carrier is large enough to achieve a constant carrier concentration over the film thickness, the charge carriers diffuse throughout the thickness (d) of the absorber, then the excess carrier concentration is

$$\Delta n = \frac{\phi\tau}{d} \tag{2}$$

and the charge balance is $np = \frac{\phi\tau}{d} N_A$, with n, p and N_A being the electron concentration, hole concentration and doping concentration respectively. Then, the dependence of doping concentration on the quasi-Fermi level splitting is

$$\frac{\phi\tau}{d} N_A = n_i^2 \exp\left(\frac{\Delta E_F}{K_B T}\right) \tag{3}$$

where, n_i is the intrinsic carrier concentration, ΔE_F is the quasi-Fermi level splitting, K_B is the Boltzmann constant and T is the temperature in Kelvin. The electron and hole effective masses of 0.16 m_0 and 1.3 m_0 respectively, m_0 being the free electron mass, for $CuInS_2$ as given by Binsma *et al* [31] to calculate the intrinsic carrier concentration are utilized. These constants, together with the measured opto-electronic quantities of effective lifetime and QFLS, allows the estimation of the doping concentration of the p-type absorbers.

The calculated doping concentration is plotted against the Cu/In ratio in figure 4. It can be observed that, the plot mirrors the figure 3(a) where QFLS is plotted against Cu/In ratio. We expect this correlation when the lifetime is constant, since then the QFLS is proportional to the logarithm of the doping concentration. For samples A, B and C with similar Cu/In ratio of 1.8, the doping concentration is seen to increase with the growth temperature. To support these series of calculations, doping concentration was also estimated from a CV measurement, performed on finished devices. Due to shunting, it was not possible to do a CV measurement on all the absorbers. However, it was found that, the absorbers processed at 650 °C, with Cu/In ratio higher than 1.4, have doping concentration in the order 10^{17} cm^{-3}, while those absorbers with Cu/In ratio ~1.3 or lower were in the order of 10^{16} cm^{-3}. These observations show that, the increase of QFLS with growth temperature or with Cu/In ratio results from higher doping concentration and not from a decrease in recombination rate.

4. Conclusion

In this work, we studied the cause of the improvement in QFLS with higher deposition temperature and higher Cu/In ratio in Cu-rich $CuInS_2$ absorbers. We showed that, although a higher absorber processing temperature and a higher Cu/In ratio in Cu-rich $CuInS_2$ absorbers lead to a significant improvement in the QFLS, these parameters do not influence the effective lifetime. Rather, the improvement in QFLS with growth temperature and Cu/In ratio, results from an increase in doping concentration, which expectedly shifts the position of the hole Fermi energy level lower and closer to the valence band. Although we previously saw a lower density of deep defects, the minority carrier lifetime is not affected by the changes in deposition temperatures and Cu/In ratio. As such, to optimize $CuInS_2$ solar cells for higher efficiency, it is still necessary to reduce the recombination channels that reduces the effective lifetime.

Acknowledgments

The authors would like to acknowledge the Luxembourgish Fonds National de la Recherche (FNR) for the funding under the framework of the MASSENA (PRIDE15/10935404) and Corrkest (C15/MS/10386094) Projects. The authors would also like to thank Michele Melchiorre from the University of Luxembourg for KCN etching.

Data availability statement

All data that support the findings of this study are included within the article (and any supplementary files).

ORCID iDs

Damilola Adeleye https://orcid.org/0000-0001-6359-9100
Alberto Lomuscio https://orcid.org/0000-0002-3356-2486
Mohit Sood https://orcid.org/0000-0002-2714-7737
Susanne Siebentritt https://orcid.org/0000-0001-6522-1427

References

[1] Tell B, Shay J L and Kasper H M 1971 Electrical properties, optical properties, and band structure of $CuGaS_2$ and $CuInS_2$ *Phys. Rev.* B **4** 2463–71
[2] Siebentritt S 2017 High voltage, please! *Nat. Energy* **2** 840–1
[3] Albrecht S and Rech B 2017 Perovskite solar cells: on top of commercial photovoltaics *Nat. Energy* **2** 1–2
[4] Hiroi H, Iwata Y, Horiguchi K and Sugimoto H 2015 960-mV open-circuit voltage chalcopyrite solar cell *IEEE J. Photovolt.* **6** 309–12
[5] Jackson P, Wuerz R, Hariskos D, Lotter E, Witte W and Powalla M 2016 Effects of heavy alkali elements in Cu (In, Ga) Se_2 solar cells with efficiencies up to 22.6%, physica status solidi *(RRL)–Rapid Research Letters* **10** 583–6
[6] Hiroi H, Iwata Y, Adachi S, Sugimoto H and Yamada A 2016 New world-record efficiency for pure-sulfide Cu(In,Ga)S_2 thin-film solar cell with Cd-free buffer layer via KCN-free process *IEEE J. Photovolt.* **6** 760–3
[7] Lomuscio A, Rödel T, Schwarz T, Gault B, Melchiorre M, Raabe D and Siebentritt S 2019 Quasi-fermi-level splitting of Cu-poor and Cu-rich Cu In S_2 absorber layers *Phys. Rev. Appl.* **11** 054052
[8] Lomuscio A, Melchiorre M and Siebentritt S 2018 Influence of stoichiometry and temperature on quasi Fermi level splitting of sulfide CIS absorber layers *2018 IEEE 7th World Conf. on Photovoltaic Energy Conversion (A Joint Conf. of 45th IEEE PVSC (WCPEC)*
[9] Unold T and Gütay L 2016 Photoluminescence analysis of thin-film solar cells. Advanced characterization techniques for thin film solar cells, photoluminescence analysis of thin-film solar cells *Advanced Characterization Techniques for Thin Film Solar Cells* **1** 275–97
[10] Würfel P and Würfel U 2016 *Physics of Solar Cells: from Basic Principles to Advanced Concepts* (New York: Wiley) (https://doi.org/10.1002/9783527618545)
[11] Ahrenkiel R K 1993 Chapter 2 minority-carrier lifetime in III–V semiconductors *Minority Carriers In III–V Semiconductors: Physics and Applications* ed R K Ahrenkiel and M S Lundstrom (Amsterdam: Elsevier) pp 39–150
[12] Ohnesorge B, Weigand R, Bacher G, Forchel A, Riedl W and Karg F H 1998 Minority-carrier lifetime and efficiency of Cu(In,Ga)Se2 solar cells *Appl. Phys. Lett.* **73** 1224–6
[13] Maiberg M, Hölscher T, Zahedi-Azad S, Fränzel W and Scheer R 2015 Investigation of long lifetimes in Cu(In,Ga)Se_2 by time-resolved photoluminescence *Appl. Phys. Lett.* **107** 122104
[14] Metzger W K, Repins I L and Contreras M A 2008 Long lifetimes in high-efficiency Cu(In,Ga)Se_2 solar cells *Appl. Phys. Lett.* **93** 022110
[15] Kim S, Nagai T, Tampo H, Ishizuka S and Shibata H 2020 Large open-circuit voltage boosting of pure sulfide chalcopyrite Cu(In,Ga)S_2 prepared using Cu-deficient metal precursors *Prog. Photovoltaics Res. Appl.* **28** 816–22
[16] Mora S, Romeo N and Tarricone L 1979 Minority carriers lifetime measurements in $CuInS_2$ by photoelectromagnetic effect *Solid State Commun.* **29** 155–7
[17] Schroder D K 2015 *Semiconductor Material and Device Characterization* (New York: Wiley) (https://doi.org/10.1002/0471749095)
[18] Sze S M and Ng K K 2006 *Physics of Semiconductor Devices* (New York: Wiley) (https://doi.org/10.1002/0470068329)
[19] Werner F 2017 Hall measurements on low-mobility thin films *J. Appl. Phys.* **122** 135306
[20] Abou-Ras D, Kirchartz T and Rau U 2016 *Advanced Characterization Techniques for Thin Film Solar Cells* (New York: Wiley) (https://doi.org/10.1002/9783527699025)
[21] Weber M, Scheer R, Lewerenz H, Jungblut H and Störkel U 2001 Microroughness and composition of cyanide-treated $CuInS_2$ *J. Electrochem. Soc.* **149** G77
[22] Regesch D, Gütay L, Larsen J K, Deprédurand V, Tanaka D, Aida Y and Siebentritt S 2012 Degradation and passivation of $CuInSe_2$ *Appl. Phys. Lett.* **101** 112108
[23] O'Connor D V and Phillips D 1984 *Time-correlated Single Photon Counting* (London; Orlando: Academic) (https://doi.org/10.1016/B978-0-12-524140-3.X5001-1)

[24] Scheer R and Schock H-W 2011 *Chalcogenide Photovoltaics: Physics, Technologies, and Thin Film Devices* (New York: Wiley) (https://doi.org/10.1002/9783527633708)

[25] Maiberg M and Scheer R 2014 Theoretical study of time-resolved luminescence in semiconductors: II. Pulsed excitation *J. Appl. Phys.* **116** 123711

[26] O'Connor D, Ware W and Andre J 1979 Deconvolution of fluorescence decay curves. A critical comparison of techniques *J. Phys. Chem.* **83** 1333–43

[27] Sood M, Elanzeery H, Adeleye D, Lomuscio A, Werner F, Ehre F, Melchiorre M and Siebentritt S 2020 Absorber composition: a critical parameter for the effectiveness of heat treatments in chalcopyrite solar cells *Prog. Photovoltaics Res. Appl.* **28** 1063–76

[28] Redinger A, Levcenko S, Hages C J, Greiner D, Kaufmann C A and Unold T 2017 Time resolved photoluminescence on Cu(In, Ga)Se_2 absorbers: distinguishing degradation and trap states *Appl. Phys. Lett.* **110** 122104

[29] Wurfel P 1982 The chemical potential of radiation *J. Phys.* C **15** 3967

[30] Babbe F, Choubrac L and Siebentritt S 2016 Quasi Fermi level splitting of Cu-rich and Cu-poor Cu (In, Ga) Se_2 absorber layers *Appl. Phys. Lett.* **109** 082105

[31] Binsma J, Giling L and Bloem J 1982 Luminescence of $CuInS_2$: II. Exciton and near edge emission *J. Lumin.* **27** 55–72